Chemoattraction and Chemotaxis in *Dictyostelium discoideum*: Myxamoeba Cannot Read Spatial Gradients of Cyclic Adenosine Monophosphate

MICHAEL G. VICKER, WALTER SCHILL, and KARSTEN DRESCHER
Departments of Biology and Mathematics, University of Bremen, D-2800 Bremen 33, Federal Republic of Germany

ABSTRACT Myxamoebae of the morphogenetic cellular slime mold *Dictyostelium discoideum* are thought to be able to accurately read and respond to directional information in spatial gradients of cyclic AMP. We examined the spatial and temporal mechanisms proposed for chemotaxis by comparing the behavior of spreading or evenly distributed cell populations after exposure to well-defined spatial gradients. The effects of gradient generation on cells were avoided by using predeveloped gradients. Qualitatively different responses were obtained using (*a*) isotropic, (*b*) static spatial, or (*c*) temporal (impulse) gradients in a simple chamber of penetrable micropore filters. We simulated models of chemotaxis and chemokinesis to aid our interpretations. The attractive and locomotory responses of populations were maximally stimulated by 0.05 μM cyclic AMP, provided that cellular phosphodiesterase was inhibited. But a single impulse of cyclic AMP during gradient development caused a greater and qualitatively different attraction. Attraction in spatial gradients was only transient, in that populations eventually developed a random distribution when confined to a narrow territory. Populations never accumulated nor lost their random distribution even in extremely steep spatial gradients. Attraction in spatial gradients was inducible only in spreading populations, not randomly distributed ones. Thus, spatial gradients effect biased-random locomotion: i.e., chemokinesis without adaptation. Cells cannot read gradients; the reaction of the cells is stochastic. Spatial gradients do not cause chemotaxis, which probably requires a sharp stimulant concentration increase (a temporal gradient) as a pulse or impulse. The results also bear on concepts of how embryonic cells might be able to decipher the positional information in a morphogen spatial gradient during development.

The morphogenesis of free-living myxamoebae of *Dictyostelium discoideum* into a differentiated metazoan is characterized by the intermingling effects of cyclic AMP (cAMP), including increased cohesiveness, chemokinesis, chemotaxis, cell polarization, cAMP and cAMP phosphodiesterase (PDE)[1] synthesis and emission, aggregation, and differentiation (1–8). The aggregation of dispersed populations follows starvation and depends partly on the reception and excretion of cAMP by each cell. Emissions first appear in a pulsatile form and cause the orientation of individual cells (3, 9), but they later coalesce into streams, which efficiently guide them toward the aggregation center. Such morphogenic fields (10) might be indispensable determinants of cell positioning, patterning, and organismal form during embryogenesis (11, 12). However, the mechanisms of directed locomotion and their relation to the effect of morphogens on cells remain largely unclear.

The possible mechanisms of chemotaxis are prevalently discussed in terms of two general classes. The first class mechanisms is spatial in which individual cells sense the polarity of a stimulant gradient across their own length. The gradient must be steep enough to satisfy the cellular requirements of sensitivity, and cells must have at least two sensor positions (1, 13–15). On the basis of receptor kinetics, cells such as bacteria or amoebae are theoretically capable of sensing gradients (16), albeit over discrete periods of ~1 s or

[1] *Abbreviations used in this paper:* BBSS, Bonner's buffered salt solution; DTT, dithiothreitol; PDE, phosphodiestease; SM medium, Sussman's standard medium; ϕ, diameter.

THE JOURNAL OF CELL BIOLOGY · VOLUME 98 JUNE 1984 2204-2214

~20 s, respectively. Spatial sensing has been proposed to account for the taxis of leukocytes, leukocyte fragments (17), and the myxamoebae of *D. discoideum* (13, 14). The second class of mechanisms is temporal and is best illustrated by the behavior of some enterobacteria (18, 19). The relaxation properties proposed for their locomotor-stability apparatus are seen to cause adaptation to the local attractant concentration. As they swim up a gradient or plunge into a higher concentration, they tend to turn less frequently; but persistence rapidly degenerates in isotropic or decreasing concentrations. Because directional "choices" always remain random, the mechanism is in fact klinokinetic with adaptation, not chemotactic. Relatively slowly moving leukocytes and amoebae of *D. discoideum* also demonstrate (*a*) a rapid morphological and synthetic response to their respective chemoattractants and (*b*) a temporal adaptation of suitable magnitude, which might allow them to read gradients despite their leisurely pace (3, 20–30). Gerisch et al. (9) have suggested that pseudopods of *D. discoideum* might probe the environment with the ability to "read" a gradient signal. However, some evidence against the role of an adaptation process in directed locomotion has been reported by Zigmond and Sullivan (30) and is implied in other results (3, 28).

Virtually every recent discussion of directed cell locomotion has employed three additional assumptions about the mechanism cells might use to control their behavior: (*a*) the stimulant signal is effective as a spatial gradient (1, 31) or a "fixed, stable gradient" (3); (*b*) cells align accurately to the gradient by chemotaxis, which causes their attraction and accumulation (3, 9, 32–34); and (*c*) the response only operates at the level of the individual cell (3, 35). Our purpose here is to attempt to investigate these assumptions.

We chose the social myxamoeba *D. discoideum* in order to examine the mechanisms of chemoattraction and chemotaxis. We reasoned that if individual cells react accurately to directional information presented in spatial gradients of their natural chemoattractant cAMP, they would accumulate at optimal or maximal attractant concentrations. Alternatively, if cells cannot read the gradient, they should proceed to move randomly and to distribute themselves randomly on the available substrate (see reference 36, pp. 51–52).

MATERIALS AND METHODS

Cell Culture: *D. discoideum*, NC-4(H), was grown in shaken suspension at 21°C with *Escherichia coli* B/r as food (37) in 50 ml of Sussman's standard medium [SM] medium (40% in Bonner's salt solution buffered with 18 mM Na-K phosphate, pH 6.2 [BBSS]). After 48 h, cells were centrifuged, washed free of bacteria at 2°C in water, plated onto 1% agar in BBSS to give 2 × 10^6 cells/cm^2, and excess liquid was removed. Cultures were kept 17 h at 6°C until they reached the early aggregative stage.

Cell Carrier Filters and Experiments: Nitrocellulose micropore filters (5-μm pore φ, nominal thickness 150 μm; Sartorius, Göttingen, Federal Republic of Germany) were cut by a razor blade either as cell carrier strips, 150–330 μm wide and 20 mm long, or as carrier pads, 7 × 20 mm, or as migration pads, 9 × 14 mm, and were soaked 17 h in water. About 10^5 cells/mm^2 were added to dishes containing carrier filters. Some penetrated the filter within 20 min at 21°C, but incubation was continued 1 h in 10^{-9} M cAMP in BBSS to allow development of an even, moderately dense cell distribution.

Glass chambers were made by cementing coverslip pieces onto microscope slides (Fig. 1*A*). The wells for attractant or sink (5 × 5 × 25 mm) were separated by a 3-mm air gap. Each well was filled with 400 μl of BBSS with or without cAMP (Sigma Chemical Co., Munich, Federal Republic of Germany), and a migration pad was laid across the gap and held fast by the liquid in each well. Gradients were developed 1 h on ice until virtually linear and free of perturbations (38). Subsequently, a cell-impregnated carrier strip (its narrowness restricted the initial position of the population) was rinsed in ice-cold BBSS, drained on damp, ice-cold filter paper, and laid along the axis of a migration pad equidistant from each well. The chambers were then incubated at 21°C for cell migration, after which the carrier strips were fixed in place with small drops of 50°C molten 1% agar, immersed in 5% formalin for 24 h, stained in Giemsa, dried (strip-side down on a microscope slide to avoid curling), cleared, and mounted in Permount (Fisher Scientific Co., Pittsburgh, PA). Cell positions were measured on a focal plane within the migration pad in 4–6 fields/pad using a × 10 or × 16 objective and an ocular grid.

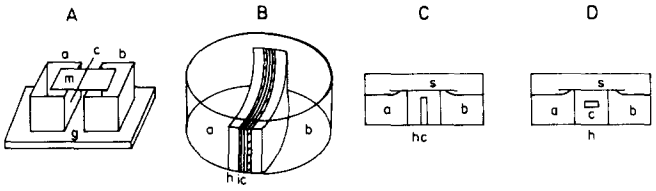

FIGURE 1 Gradient chambers: (*A*) The penetrable microfilter migration pad (*m*) spans a gap (*g*) between two wells (*a* and *b*) containing BBSS with or without cAMP. Once the cell-laden carrier strip (*c*) is in place, the chambers are incubated in 100% humidity. (*B*) Two carrier filter pads (*c*) are juxtaposed between either two migration pads (not shown) and/or two impenetrable border pads (*i*). The assembly is pressed between two 2-mm slabs (*h*) of 1% agarose or two layers of three micropore filters (450 μm thick) and bowed, then it is sealed across a 35-mm φ Petri dish forming a source and a sink compartment (*a* and *b*). (*C*) A side view of a 5 mm wide barrier (*h*) of 1% agarose in BBSS, which spans a plastic, tissue culture Petri dish (35-mm φ). A cell suspension is drawn into the ~100-μm-wide slit (*c*), and the cells settle and crawl on the dish under the agarose. A coverglass (*s*) levels the source and sink (*a* and *b*) at the block and improves its optical quality. (*D*) Cells were drawn into the narrow (<1 mm), low chamber (*c*) within the 3 mm wide barrier (*h*), as shown in C. Gradient development as described in the text.

To test whether cells could read cAMP gradients, the territory available for cell locomotion was limited to 150, 300, or 600 μm (Fig. 1*B*). Small dimensions were necessary, because of the slow rate of spread and progressive differentiation of populations. Territories 300 μm wide were created by juxtaposing two carrier pads at their originally plated surfaces. Each pad was permeated with cells, rinsed, and drained as before. The pair was placed between two nitrocellulose filter "borders" (0.45-μm pore diameter [φ]), which blocked cell passage. Other assemblies included a 5-μm pore φ migration pad between each carrier and border filter pad. Assemblies were sandwiched between either two 2-mm-thick slabs of 1% agarose (Pharmacia, Freiburg, Federal Republic of Germany) in BBSS or two layers of three micropore filters (12-μm pore φ), which stabilized a moderate gradient. Complete assemblies were placed across the diameter of 35-mm φ plastic Petri dishes, bowed slightly to press the filters together, and then sealed onto the dish with molten agarose. These steps were conducted on ice to prevent cell movement. The wells were filled with 2.5 ml ice-cold BBSS with or without cAMP, and the gradient was developed 2 h on ice until virtually static and linear, remaining unperturbed and undiminished for a further 4 h (38). Care was taken to assure equal access of air to each side of assemblies (39). Dishes were warmed to 21°C for cell movement. After fixation, staining, and mounting, the cell distributions were measured in consecutive optical sections (40) through the depth of the filter, beginning 4 μm beneath the surface to avoid immotile cells. A × 40 objective was used to count four to seven fields/pad at comparative positions between pads. Cells out of focus between sections were ignored, but none was counted twice. We also ignored cells attached to the border surface, but this did not affect the results.

Direct Observation of Cells in cAMP Gradients: Cells were confined to a narrow vertical slit formed under a 5-mm-wide block of 1% agarose, which spanned a 35-mm φ tissue culture plastic Petri dish (Falcon, Heidelberg, Federal Republic of Germany) as in Fig. 1*C*. The cells settled onto the dish surface during cAMP gradient development for 2 h at 2°C. The slit was created by molding a 100-μm-thick coverslip into the agarose and removing it after gelation.

We also created completely enclosed chambers within agarose blocks (Fig. 1*D*). A long, narrowing sliver of a coverslip was molded, broad side horizontally, in 1% agarose in BBSS. Withdrawl of the sliver sucked a cell suspension into the ~1-mm-wide gap within the 3-mm-wide agarose block. This was sealed across the diameter of a Petri dish, and a cAMP gradient was developed at 2°C. The collapse of the chamber roof onto the floor reduced the area to essentially two dimensions, but did not impede cell locomotion. Periodically, the cell

positions were measured microscopically using a × 10 objective and an ocular grid.

Delivery of cAMP Gradients: Starving myxamoebae respond to cAMP pulses by expressing PDE on their surface and excreting cAMP and another PDE (2, 41–43). During development the cell surface PDE is inhibited while the extracellular variety increases (37, 42, 44, 45). We used early aggregative-stage cells to reduce the presence of the latter PDE. Both PDE expression and cAMP excretion are inhibited by the continuous presence of cAMP (20, 21, 43, 44, 46). We also included 1–2 mM dithiothreitol (DTT, Boehringer, Mannheim, Federal Republic of Germany) in all incubation media to suppress the enzyme's activity (21, 44, 47 and Table I). Concentrations of cAMP were measured using a test kit (Amersham, Amersham, England).

To eliminate the effects of the temporal gradient during gradient generation, we cooled cells on ice throughout gradient development for 1–2 h. This technique assures that cellular responses were elicited only by the static spatial gradient. Cellular reactions such as locomotion are inhibited, and adaptive reactions to cAMP addition (3, 24, 29) will be completed before incubation at 21°C. In this work the term spatial gradient indicates the absence of the effects on cells of gradient development.

In spatial linear gradients the proportional concentration difference across the length of each cell, $\Delta c/c$, varies inversely with the distance from the source of attractant: $\Delta c/c = l/(L - d)$, where c is concentration of stimulant, l is cell length along the gradient, L is length of the gradient and d is distance of the cell from c_{max}. For example, assuming l is 15 μm, L is 3,000 μm, and d is either 100, 1,500 or 2,900 μm, then for any gradient $\Delta c/c$ is 0.52, 1.0, and 15%, respectively. Thus, cells encounter weaker directional information (as $\Delta c/c$) as they ascend linear gradients; in exponential gradients the value of Δc across a cell increases and that of $\Delta c/c$ remains constant as it nears the source (1).

Computation and Analysis: For each experiment and simulation we calculated a one-dimensional distribution of cells in grouped form and evaluated the distribution characteristics, viz., mean, median, standard deviation and skew (see Appendix *A*). Each experiment was repeated at least three times. In most cases all cells started from the central 0 position. If they move randomly one should expect a symmetrical distribution about 0. Therefore, we interpreted movements of the mean and median as indicators of a shift in the population. The standard deviation serves as a measure for the dispersion (migration) of cells (note, however, that the standard deviation is bounded because the territory for locomotion is bounded), and skewness is an indicator of symmetry. By convention, a negative sign indicates a shift up-gradient for the mean and median. We performed a signed rank test to examine the significance of the median shift: Xnorm is normally distributed; Xnorm < −2.58 (>2.58) indicates a shift to the left, i.e., up-gradient (to the right, i.e., down-gradient) at the 1% level of significance (Appendix *B*).

RESULTS

Attraction in Static Gradients

Under conditions where stimulant gradients develop without perturbation, such as in a gel, populations of spreading leukocytes (48, 49) and confined *D. discoideum* myxamoebae (14, 50) form a characteristic shifted spatial-distribution pattern. This behavior is clearly seen (Fig. 2) as cells emerge from a narrow confine under a barrier of agarose (as in Fig. 1*C*) in a predeveloped spatial cAMP gradient. The shift in the mean and median cell position started upon incubation at 21°C and continued for over 3 h (Fig. 3, Table II).

A similar distribution pattern forms as myxamoebae migrate from the confines of a narrow microfilter carrier strip into the labyrinth of a microfilter migration pad (Fig. 1*A*) containing a predeveloped spatial cAMP gradient (Fig. 4, upper panel). We term this pattern of up-gradient population shift chemoattraction. It becomes evident when a population is confronted essentially with only a spatial gradient, requiring that the effects of gradient development are eliminated.

Attraction in a Developing Gradient

We examined the difference between the effects of static, spatial gradients and developing (temporal) gradients by subjecting migrating populations to an impulse of cAMP. The source well on the left of the migration pad was filled immediately after the cell carrier strip was in place at 21°C. The response of the population far exceeded that in static, predeveloped gradients even though the gradient here had not existed so long (Fig. 4, lower panel). The results demonstrated two important differences between the two treatments. (*a*) Most migration took place at a higher, less attractive (see

TABLE I

Gradients of cAMP in the Presence and Absence of DTT

	Control	Cells added	Cells and 2 mM DTT added
		pmol/aliquot	
Source	17.01 (1.92)	9.30 (1.46)	15.98 (4.06)
Sink	1.38 (0.181)	0.244 (0.196)	1.51 (0.323)
cAMP loss	—	−48.12%	−4.89%

1.6×10^5 amoebae were plated at 10^4/mm² on micropore filters, which connected source and sink wells 5 mm apart as in Fig. 1*A*. Cells were omitted in the control. 3.3×10^{-7} M cAMP was added to each source well and BBSS to each sink. 50-μl aliquots were withdrawn for cAMP measurement after 270 min. The values are given as pmol/aliquot with ± standard deviation (n = 7 for sink and 4 for source) in parentheses. Losses of cAMP are comparisons of total cAMP/ml to that in the control.

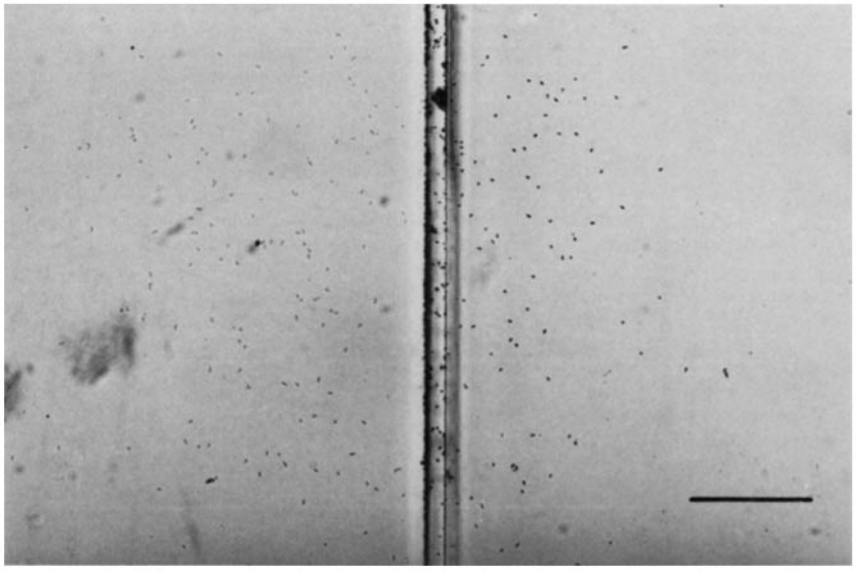

FIGURE 2 Migration of myxamoebae under agarose in a cAMP gradient (see Fig. 1C) viewed from above. The gradient was predeveloped on ice 2 h before the cells in the central, vertical slit (87 μm wide) were allowed locomotion at 21°C for 200 min. Two wells, each 2.5 mm from the slit, contained 2.5×10^{-7} M cAMP on the left and BBSS alone on the right (i.e., 0.05 μM/mm). DTT was not present. Panatomic X (Kodak) was used with green filter and a 2.5× objective without condensor on a Zeiss inverted microscope. Bar, 500 μm. × 333.

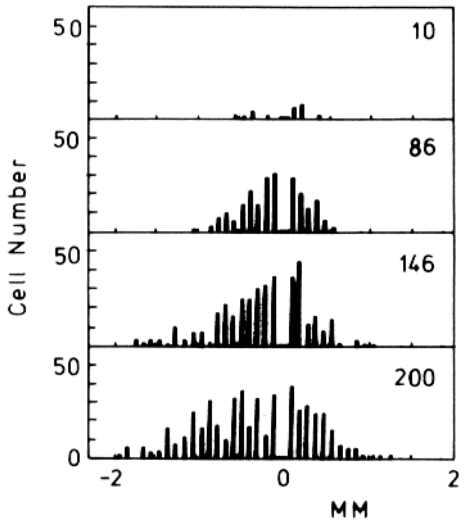

FIGURE 3 Chemoattraction of a spreading myxamoeba population in a cAMP gradient. The cell positions are from a series of photographs from the experiment in Fig. 2. The population spreads from the slit (position 0) and shifts toward the cAMP source on the left. The incubation time in minutes is given in the upper right corner of each panel. Each bar is 100 μm apart on the x axis.

TABLE II

Chemoattraction of Myxamoebae in a Static cAMP Gradient under Agarose

Time	n	Median	Mean	SD	Skew
min		*mm*	*mm*	*mm*	
10	13	0.050	−0.046	0.328	−0.43
86	111	−0.090	−0.137	0.371	−0.22
146	195	−0.159	−0.252	0.563	−0.44
200	252	−0.269	−0.322	0.680	−0.14

The data refer to Fig. 3. *n* is number of cells at all positions excluding the slit. Standard deviation (SD) of the mean is an indication of the degree of spread or migration. Negative values correspond to movement up the cAMP gradient.

below) mean cAMP concentration than in the static control, because the starting position of the cells was nearer the cAMP well. (*b*) More significantly, while populations in static gradients always remained distributed about the original mean position, impulsed populations shifted *en masse* up-gradient. However, in this example and in one other case, a minor group of cells moved down-gradient. We cannot explain this behavior, but similar patterns are evident in the experiments of others under analogous circumstances (14, 50). We have no way of eliminating the single brief stimulated excretion of cAMP by cells after the cAMP impulse. Excretion might amplify the effect of the original impulse, but cannot cause the attraction here. Since PDE activity was suppressed, the mean cAMP concentration would have risen about the cells, thus decreasing gradient steepness.

Effect of cAMP Concentration

An essentially one-dimensional analysis of cell distribution patterns (e.g., Fig. 2) may be used to quantitatively compare the effects of different cAMP concentration (Fig. 5). The shifts of mean and median and the degree of migration (related to the standard deviation of the mean) indicate that cells are most reactive to about 5×10^{-8} M cAMP: a concentration that also induces the half-maximal cAMP signalling response (21), half-maximal binding of cell-surface cAMP receptors,

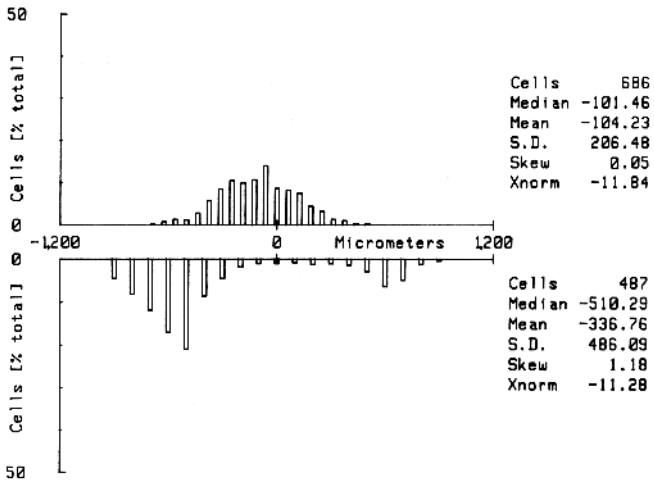

FIGURE 4 Attraction and population distribution of myxamoebae spreading in a micropore filter. *Upper* panel: a static predeveloped linear gradient spans a migration pad from 10^{-6} M cAMP at −1,500 μm (0.33 μM/mm over 3 mm, $\bar{c} = 5 \times 10^{-7}$ M at x_0). As in Fig. 1*A*, a cell laden carrier strip 260 μm wide was placed at x_0 and cell positions recorded after 105 min incubation. Bars are 62.5 μm apart. *Lower* panel: the effect of a cAMP impulse. As above, but 10^{-6} M cAMP was added to the well on the left after the carrier strip was in place at 21°C. x_0 is 0.7 mm from C_{max}. Incubation was stopped at 60 min. Bars are 100 μm apart.

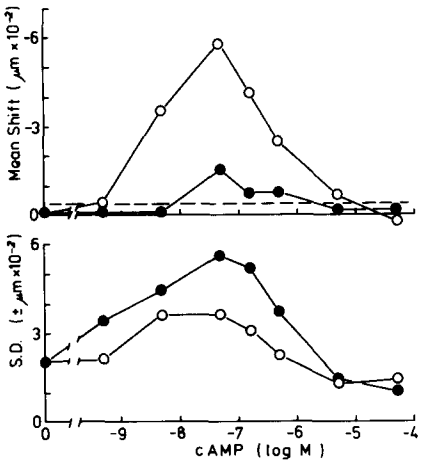

FIGURE 5 The attraction and migration of myxamoebae in response to differing cAMP concentrations. The experiment was as in Fig. 4 (*upper* panel). The cAMP values are those equidistant between wells at the carrier strip position. A negative mean shift in gradients indicates attraction, and S.D. of the mean is related to migration. Mean shifts in isotropic cAMP concentrations (●) are all presented as negative, and the dashed line marks the average shift of all such populations. Only those values at 5×10^{-8} M and 5×10^{-7} M are significant at the 1% level. Mean shifts in gradient cultures (○) are significant at the 1% level for 5×10^{-9}, 5×10^{-8}, 1.6×10^{-7}, and 5×10^{-7} M cAMP.

and maximal binding of intracellular cyclic guanosine monophosphate (29) in the presence of DTT. Without DTT the requirement for cAMP is about 10-fold higher for maximal attraction (our unpublished observations). Migration in spatial gradients is consistently less than in isotropic concentrations, but the response pattern is similar in each case. Some inhibition of migration is apparent at the higher cAMP concentrations.

We used mean cAMP concentrations of 5×10^{-7} M in most experiments, although it gave less than maximal attrac-

tion, because high concentrations suppress autonomous cAMP signaling. They also protect the gradient against residual PDE activity, especially during long incubations (Table I). However, lower cAMP concentrations, with and without DTT, gave similar results.

Possible Causes of Shifted Distributions

The development of the population distribution pattern and the attraction observed in static, spatial cAMP gradients might be determined or affected by three factors or mechanisms, which we examined.

(*a*) Myxamoebae might behave as two subpopulations, one of which is an inherently insensitive or incompetent gradient reader. For example, prespore and prestalk cells in late aggregation-stage cultures demonstrate different degrees of chemotaxis (51, and see reference 52), which might cause "sloppy" distributions. Therefore, we examined cells which had moved either up- or down-gradient. First, the cells were separated by trapping them in carrier strips, which were placed at the *i* position in filter assemblies as in Fig. 1 *B*. Each strip was then placed upon migration pads in predeveloped cAMP gradients as in Fig. 1 *A*. The mean and median shifts and the standard deviation of each subpopulation were comparable and also similar to those of an intact population (Fig. 6). Thus, the distribution pattern is probably not due to any inherent population inhomogeneity.

(*b*) Cells might become progressively insensitive to cAMP gradients over long exposure times leading to sloppy distributions. The endurance of the attractive response was examined by preincubating cells in carrier strips 120 min in a cAMP gradient and then placing each strip upon a migration pad in a fresh gradient as in Fig. 1 *A* for 90 min (Fig. 7). There was no evident diminution of the attractive response after exposure to cAMP and DTT for 210 min. Indeed, during cell development the chemotactic response reportedly increases (3).

(*c*) The attractive distribution pattern reflects two components of locomotion: random motility and a superimposed chemotactic drift (e.g., reference 53, cf. reference 13).

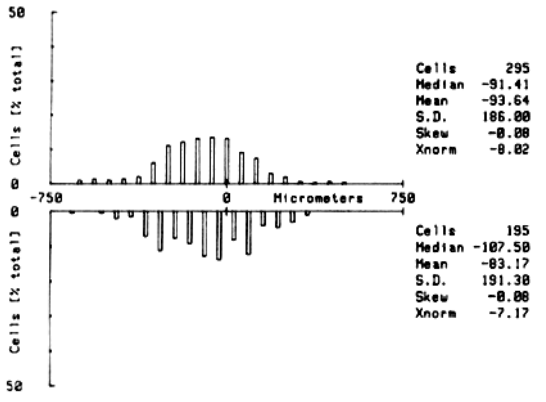

FIGURE 6 Comparative attraction of up-gradient and down-gradient populations. To divide a population, we placed two cell-laden carrier pads together between empty carrier strips (as in Fig. 1 *B*) each ~300 μm wide. The assembly was placed ice-cold between two blocks of 1% agarose, one of which contained 5×10^{-7} M cAMP ($\bar{c} = 2.5 \times 10^{-7}$ M at x_0 and 8.3×10^{-7} M/mm over 0.6 mm), and warmed to 21°C after 30 min. The up- and down-gradient strips were removed after 30 min and laid on fresh migration pads in a predeveloped cAMP gradient as in Figs. 1 *A* and 4 and incubated 105 min at 21°C. *Upper* panel: positions of up-gradient cells, *lower* panel: those of down-gradient cells. Bars are 62.5 μm apart.

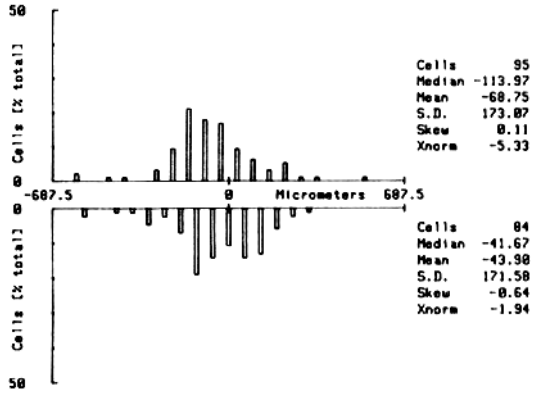

FIGURE 7 Endurance of the attraction response. *Upper* panel: cells were preincubated for 2 h at 21°C in carrier strips suspended between two wells containing 10^{-6} M cAMP. Each strip was then placed upon a migration pad as in Fig. 1 *A* and incubated in a predeveloped gradient 90 min (10^{-6} M cAMP at −2,500 μm giving 0.2 μM/mm over 5 mm). *Lower* panel: no preincubation. Bars are 62.5 μm apart.

Confined Populations in Gradients

Cells that detect and respond to the direction of a cAMP spatial gradient, either by chemotaxis or by chemokinesis with adaptation (whatever the mechanism), ought to accumulate. Therefore, the shift in the mean cell position (cf. Fig. 2) ought to increase steadily and irreversibly. Alternatively, cells that cannot read gradients are thought to move randomly (36). If allowed to invade new territory they should distribute themselves randomly about their initial position, because of their random locomotion. Cells that are initially randomly spread over a bounded or an infinite territory should remain so, whereas gradient-reading cells will still accumulate. However, consider an analogy in which some water is quickly poured between two compartments in a level container. The compartment on the left has a large hole in its wall and that on the right a small hole. Initially, most of the water will flow to the left, then retreat, and the water "mean position" will eventually equilibrate at 0: exactly between the compartments. Thus, even without taxis a temporary sort of "attraction" occurs. Because myxamoeba populations demonstrate attraction in static gradients of cAMP, can the cells read the spatial gradient?

We sought to answer this question using two complimentary test conditions in bounded territories. Cells were exposed to spatial gradients either (*a*) as they invaded fresh territory or (*b*) as an already randomly spread population. Unlimited spreading was impractical; therefore, we confined the territory available to cells to the depth of one or a few micropore filter pads in a cAMP gradient (as in Fig. 1 *B*). Cells that migrated out of the two central carrier pads into the neighboring migration pads assumed initially the characteristic up-gradient shift in their distribution (Fig. 8, *upper* panel). The cAMP concentration used here is similar to that detected in naturally aggregating populations (54). Yet, within 150 min, as the population filled the territory, the mean and median cell positions had retreated, and the population distribution became virtually symmetrical about x_0 (Fig. 8, *lower* panel). Even after 4 h there was never evidence of accumulation.

We examined whether such symmetrical distributions

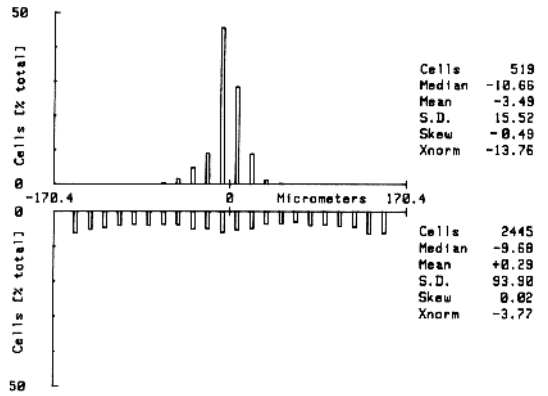

FIGURE 8 Chemoattraction by cAMP in a confined territory leads to an even population distribution. Experiments were as in Fig. 1 *B*, but the cells could wander through migration pads before reaching the territorial borders. After development of linear, static gradients (10^{-6} M cAMP at −900 μm giving 0.56 μM/mm over 1.8 mm, $\bar{c} = 5 \times 10^{-7}$ M), cultures were incubated at 21°C. Carrier pad positions are at $x = 0$. *Upper* panel: cell positions in the migration pads after 15 min incubation, *lower* panel: the distribution after 150 min. Bars are 14.2 μm apart.

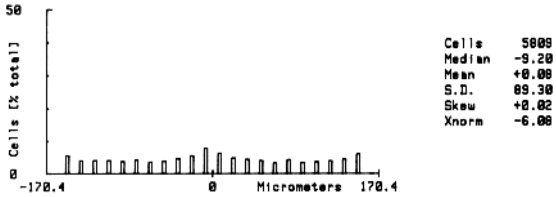

FIGURE 9 Confined, evenly distributed myxamoeba populations are not attracted when exposed to static cAMP gradients. Two evenly laden cell carrier pads were sandwiched between two border pads as in Fig. 1 *B*. After gradient development (10^{-6} M cAMP at −750 μm and $\bar{c} = 5 \times 10^{-7}$ M giving 0.67 μM/mm over 1.5 mm), cells were able to locomote at 21°C for 150 min. Cell positions are recorded in the carrier pads at 14.2-μm intervals.

might arise artifactually: e.g., because of the long incubations, the effects of exposure to DTT, incubation times too short to allow accumulation, or cell interactions such as population effects (52) that might make a random distribution inertially or otherwise resistant to deformation. Therefore, we "inverted" the experiment in Fig. 8 by exposing an already evenly distributed cell population to a predeveloped cAMP gradient. The cells were trapped in two carrier filter pads as in Fig. 1 *B*, so the entire territory was limited to 300 μm. After 150 min incubation at 21°C there was no accumulation or evident shift in the population, which remained evenly distributed (Fig. 9). The stability of the distribution was neither artifactual nor irreversible, because a single cAMP impulse disrupted the distribution and induced attraction (Fig. 10, *lower* panel). Such disturbed populations eventually reverted to even distributions. Konijn (50) and Mato et al. (14) also found that confined myxamoeba populations were attracted if the cAMP was delivered in pulses. Thus, a qualitative difference exists between the effects of spatial and temporal gradients.

We attempted to interfere with the stability of even population distributions by exposing them to predeveloped gradients 10-fold steeper than the 0.67 μM cAMP/mm of Fig. 9, and where $\Delta c/c$ reached a value of 20% across the length of a cell at x_0. Such extreme gradients did not shift the population, which retained distribution patterns comparable to controls in isotropic cAMP (Fig. 11). We could not detect any

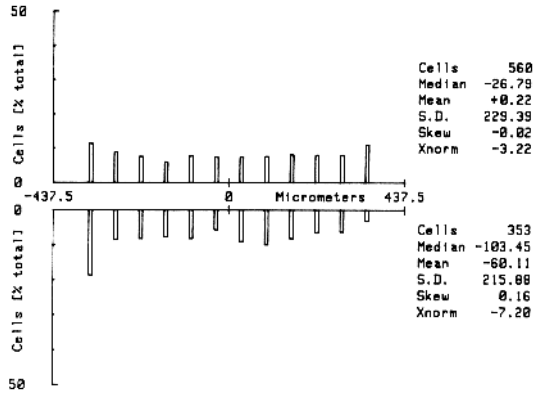

FIGURE 10 A single cAMP impulse causes attraction of cells in confined, evenly distributed populations. Locomotion chambers (Fig. 1 *A*) employed impenetrable, 0.45-μm pore φ microfilters rather than a migration pad. An evenly laden cell carrier strip 750 μm wide was placed at $x = 0$. *Upper* panel: the gradient was predeveloped (10^{-6} M cAMP at −1,500 μm giving 0.33 μM/mm over 3 mm, $\bar{c} = 5 \times 10^{-7}$ M), *lower* panel: cAMP was added after carrier strip implacement. Incubation at 21°C for 45 min. Cells refrain from leaving the carrier strip. Bars are 62.5 μm apart.

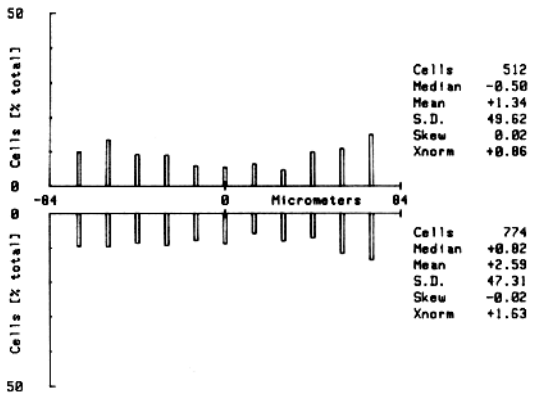

FIGURE 11 Confined myxamoeba population distributions in isotropic cAMP concentrations resemble those in steep spatial gradients. Gradients were predeveloped 15 min across 150 μm thick single carrier pads separating source and sink well (modified from Fig. 1 *B*). Cells were originally plated at $x = +75$ μm, but the pads were evenly permeated with cells before incubation at 21°C for 120 min in cAMP. *Upper* panel: 10^{-6} M cAMP left and right, *lower* panel: 10^{-6} M cAMP at −75 μm giving 6.67 μM/mm over 0.15 mm, $\bar{c} = 5 \times 10^{-6}$ M. Bars are 14.2 μm apart.

disturbances in the distribution even shortly after exposure to the gradient at 21°C (Fig. 12). Thus, it is unlikely that exposure to gradients stimulates an ephimeral, adaptive attraction. Exclusion of DTT did not affect the results. These reactions to spatial gradients indicate that the even distribution of confined populations is probably an equilibrium state due to random cell locomotion.

Although putative cell spacing or population effects might have interesting consequences in spreading and equilibrium population distributions (e.g., resisting tendencies to accumulate), they probably had no determining effect on the results for three reasons. (*a*) Strong gradients, as steep as 20% across a cell, caused no detectable accumulation. (*b*) The difference between accumulating and equilibrium populations is the presence or absence of a temporal cAMP gradient: any population effect is identical in both circumstances. (*c*) High and low population densities gave identical results; but

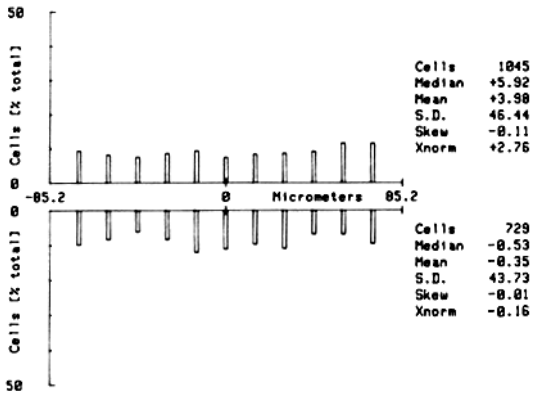

FIGURE 12 Exposure of confined, evenly distributed myxamoeba populations to static, steep cAMP gradients does not induce early attraction. Experiments were as in Fig. 11. *Upper* panel: cell distributions after 30-min incubation at 21°C, *lower* panel: after 60 min. Bars are 14.2 μm apart.

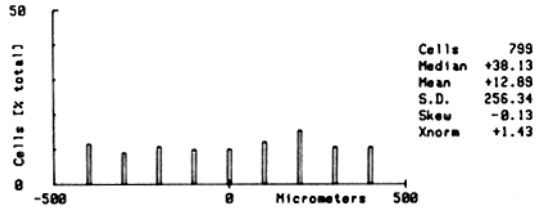

FIGURE 13 Myxamoeba populations assume virtually random distributions when confined in static spatial cAMP gradients. Cells began migration from an initial even distribution in a predeveloped, static cAMP gradient (10^{-6} M at −1,500 μm giving 0.33 μM/mm over 3 mm, $\bar{c} = 5 \times 10^{-7}$). The positions were recorded after 220 min in a 900-μm-wide horizontal slit within an agarose block as in Fig. 1*D*. Bars are 100 μm apart.

the highest density used ($<10^4$ cells/mm^2) is below the level at which known population effects become significant, i.e., $\sim 10^6$ cells/mm^2 (52).

The cell distribution tended to be distorted at filter surfaces whether in gradients or isotropic concentrations of cAMP (cf., Fig. 11). Such "edge effects" could be eliminated by confining cells to a narrow, horizontal crevice molded within an agarose block, separating a cAMP source and sink (see Fig. 1*D*). Exposure of randomly distributed populations to predeveloped, spatial cAMP gradients (Fig. 13) had no effect on their distribution, which appeared virtually random for at least several hours.

Simulations

The behavior of *D. discoideum* in static, spatial gradients of cAMP seems contrary to the current notion of chemotaxis. We compared tactic processes with a few, simple random walk models treated one-dimensionally over a finite interval of territory (−2.56 to 2.56). Particular assumptions about cell locomotion were crucial to the simulations. Thus, we stipulated that the parameters of "cell" motility were a function of their immediate position (see also reference 13). Cells that attempted to move beyond the boundaries were frustrated and remained in place: turning proceeded with the appropriate local probability, and boundaries neither reflected nor absorbed cells. Cells behaved independently of one another; their movement is assumed to be influenced by a chemoattractant, which in models *B* and *C* triggered differences in speed or persistence, respectively. The gradient had no effect on the direction of movement except in model *A*. (For more information on models *A–B*, see Figs. 14–17.) All cells started initially from 0 or were randomly distributed. In all cases the first step of each cell had an equal probability of going left or right: $P(L) = P(R)$. Cells moved with a given speed along the x axis, stopped after a fixed time and "chose" a new direction (+ or −) before proceeding. Resumption of the previous direction is persistence.

We simulated gradient model *A* by stipulating that after a step up-gradient the cell's next step is either up-gradient with $P(L) = 51\%$ or down-gradient with $P(R) = 49\%$: a Markov simulation. The model incorporates "adaptation," because after a step down-gradient, $P = 50\%$ in either direction. The simulation resulted in an initial slight shift to the left, which gradually evolved into sloppy accumulation (Fig. 14). Such weak gradient reading seems beneath the reported capabilities of leukocytes (31, 32) or myxamoebae (3, 13). It simulated sloppy accumulation in that variability between cells or between readings, whatever the mechanism, broadened the distribution. By inserting a modest 55% for $P(L)$ the initial shift was stronger, and cells accumulated tightly at the "source" (Fig. 15). The attraction in model *A* would be enhanced in the absence of the adaptation feature. We rejected model *A*

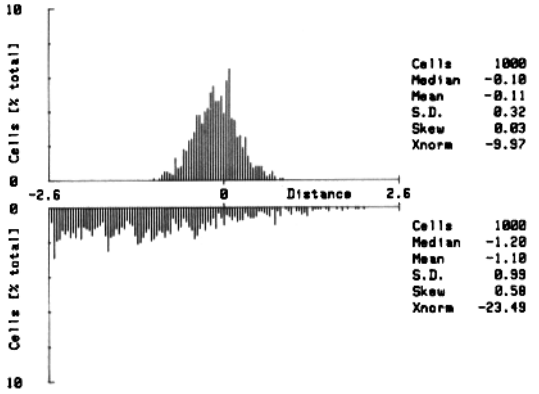

FIGURE 14 Simulation of model *A*: cells read the direction of a stimulant gradient. A linear concentration gradient decreases from $X = -2.6$ to $c = 0$ at $x = +2.6$, and all cells start at $x = 0$ at $t = 0$. For cells moving left, the probability of continuing in that direction at the next step $P(L) = 51\%$ and $P(R)$ 49%. For cells moving right, $P(L) = P(R)$ ("adaptation"). *Upper* panel: positions after 5,000 steps, *lower* panel: after 60,000 steps.

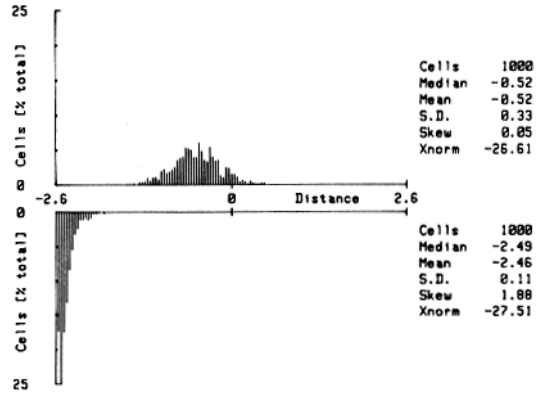

FIGURE 15 Simulation of model *A*; but for cells moving left $P(L) = 55\%$ and $P(R) = 45\%$. For cells moving right $P(L) = P(R)$. *Upper* panel: positions after 5,000 steps, *lower* panel: after 60,000 steps.

for *D. discoideum* because of the accumulation. However, by reducing the difference between $P(L)$ and $P(R)$ to a vanishingly small number, cell distributions might become impossible to differentiate from those of model *C*.

Another way to obtain accumulation is by varying cell speed with attractant concentration. Model *B* requires that $P(L) = P(R)$ everywhere, but concentration influences the cell's step-length per unit time (speed). In Fig. 16 the speed smoothly increased threefold between the minimum and maximum concentration. The mean shifted first transiently to the left, but reverted, and the population became widely spread with a slight accumulation down-gradient. Greater speed or concentration differences increased accumulation and caused repulsion, whereas effects that decrease speed caused attraction: conclusions also reached by Futrelle (13). Therefore, we rejected model *B* (as a single parameter model). Myxamoebae move faster after cAMP pulses (3), and speed has been employed in theoretical descriptions of directed locomotion (13, 55, 56).

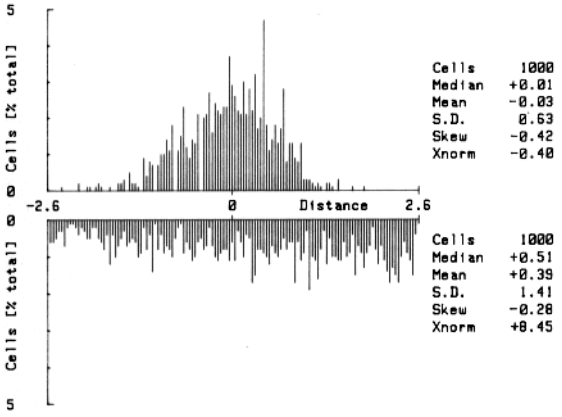

FIGURE 16 Simulation of model *B*: greater stimulant concentration increases cell speed (orthokinesis). The gradient decreases linearly from $x = -2.6$ and $P(L) = P(R)$ everywhere, but step length per unit time increases from $x = +2.6$ to $x = -2.6$ as 1:3. Cells originated at $x = 0$. *Upper* panel: distribution after 5,000 steps. Slight shifts up-gradient always occurred at first. *Lower* panel: after 60,000 steps. Identical patterns result if equally long simulations begin with random cell distributions.

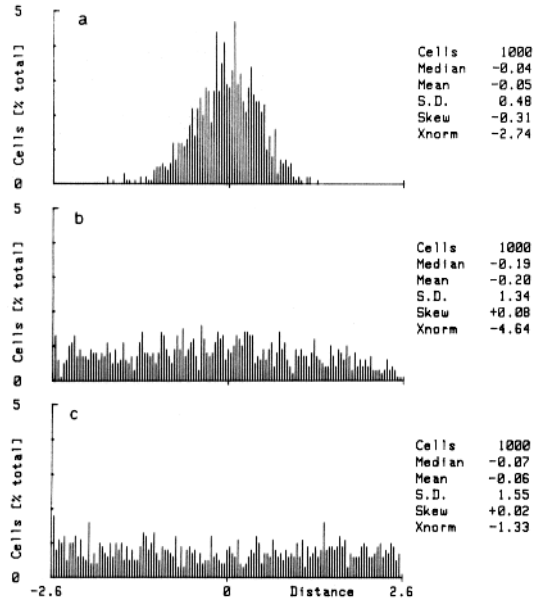

FIGURE 17 Simulation of model C: stimulants increase locomotory persistence. Speed is constant and $P(L) = P(R)$ everywhere, but $P = 50\%$ at $x = +2.6$ and decreases smoothly to 0.05% at $x = -2.6$: cells turn less frequently on the left. All cells started at $x = 0$. (*a*) Positions after 5000 steps; (*b*) the mean position shift increases after 60,000 steps; (*c*) by 260,000 steps the mean returns and fluctuates about $x = 0$. Compare Figs. 3, 4 (*upper* panel), and 8.

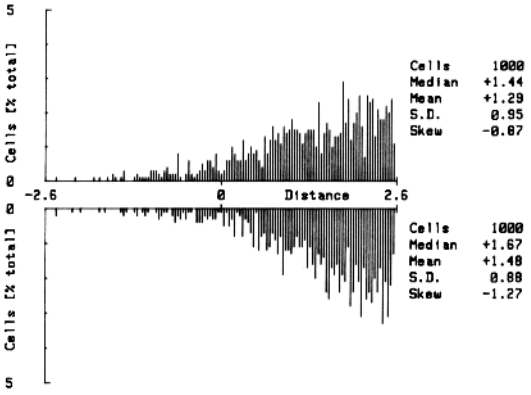

FIGURE 18 Simulated comparison of the effects of a gradient and an isotropic concentration of stimulant in the Zigmond (40) assay. All cells originate at $x = +2.6$ and move according to model C (persistence effect). The positions here were recorded after 60,000 steps. *Upper* panel: the stimulant concentration is everywhere equal to that at $x = 0$, *lower* panel: the concentration decreases linearly from $x = -2.6$. In each case, the mean positions and other differences are but quantitative.

Model *C*, a more satisfactory model, results if directional choices are random (as in model *B*), but the persistence of locomotion (one-turning frequency) increases at greater stimulant concentration. The probability of turning at the next step increases from 0.05% to 50% between C_{max} and C_{min}, regardless of the cell's momentary direction. The model is essentially klinokinesis, but lacks adaptation. Our results (Fig. 17) are virtually identical to the behavior of myxamoebae. Even in random distributions the up-gradient cells moved with greater persistence than those elsewhere, but cell losses and gains compensated each other stochastically at each point. Quantitative changes in this model did not substantially alter the results. Attraction in spatial gradients and migration in isotropic concentrations are mechanistically identical: the result of biased-random locomotion.

Zigmond and Hirsch (57) and Zigmond (40) discriminated between a stimulated random component of locomotion and a chemotactic component due to gradient reading by comparing the penetration of leukocytes into a micropore filter, bearing either a gradient or an isotropic concentration of stimulant. Our simulations (Fig. 18) demonstrate no quantitative difference in cell behavior under these two circumstances. Perhaps other factors beside the spatial gradient determined the reported differences. For example, the method of stimulant delivery might be a significant factor in such tests and, thus, in the identification of lesions in leucocyte pathology (58).

DISCUSSION

Cell Behavior in Spatial Gradients

The observations reported here are irreconcilable with previous views that a spatial gradient of cAMP in itself is capable of inducing chemotaxis in *Dictyostelium*: cell populations demonstrate neither accumulation nor, when randomly dis-

tributed, overt attraction. Thus, cells cannot interpret or read gradient polarity by either the spatial or the temporal mechanism or by temporal signal integration (16). Rather, cell migration in isotropic concentrations or spatial gradients of cAMP is determined by one and the same mechanism of chemokinesis without adaptation. Population behavior conforms to the stochastic effect of (*a*) the local cAMP concentration on (*b*) biased-random motility; the relationship is complex because it demonstrates a cAMP concentration optimum, and the relative contributions of speed and persistence components are unknown. Attraction in a spatial gradient is caused by the gradient of cell motility induced across a spreading population by cAMP; however, the same spatially graduated behavior exists, but is latent (hidden), in randomly distributed (equilibrium) populations. This form of behavior has only recently been discussed: Lapidus (55) called attention to the possibility that chemokinesis alone, in the absence of adaptation, may cause transient attraction (which he termed "pseudochemotaxis") as the distribution approaches equilibrium in a stimulant gradient. Futrelle (13) concluded that the components of locomotion in this case may appear indistinguishable from that due to taxis itself. In fact, myxamoebae demonstrate no chemotactic (or chemokinetic-adaptive) reaction to spatial gradients, because they fail to accumulate, and randomly distributed populations fail to be attracted. These views contradict those of Fraenkel and Gunn (36), who concluded that kinesis without adaptation leads only to random distribution. However, our cell and simulation observations confirm the results of Lapidus (55).

The methods used here allow scrutiny of entire cell populations. Chemotaxis, by definition, operates at the level of the individual: cells "home" accurately (3, 9, 31, 32), and regimentation is characteristic (36). But myxamoeba responses in spatial gradients are stochastic: any individual might, on the average, travel more up- than down-gradient. The chemokinetic attractive response only operates on the systematic level of summed cell paths or averaged cell (population) positions, which further differentiates it from chemotaxis.

In most investigations there persists the nearly intuitive notion that the observed cell behavior results from the specific spatial character of the applied stimulant gradient. This expectation is difficult to satisfy under experimental or, indeed, natural circumstances without precautions (36, 38), because (*a*) turbulence, convection, and molecular weight differences between stimulant and medium induce erratic perturbations, pooling, and wholesale flow of stimulant, and (*b*) such perturbations, especially those inherent in the generation of spatial gradients, confront cells as temporal gradients. The relevance of these points has been generally overlooked. Chemotaxis experiments may require reinterpretation where the nominally "fixed, stable gradient" included significant temporal components (impulses). Only a few investigators have measured the gradient development or form in their experiments (33, 38, 59, 60).

Concepts of Cell Behavior

Fraenkel and Gunn (36) rigorously differentiated (*a*) taxis—the alignment (the word means order) of individuals with the field and (*b*) kinesis—the effect of a stimulant on the speed (orthokinesis) and/or the turning (klinokinesis) of an organism, which produces biased-random locomotion. However, cause and effect may not have been adequately separated, which leads to colloquial uses of concepts (cf. reference 3, where chemotaxis is said to result from klinokinesis) if not confusion. Most investigations are not specifically designed to discriminate between orientation, attraction, or accumulation and how they are induced. For example, some commonly applied "chemotactic indices" compare relative path lengths (61), population shifts (55), or angles of approach (3), which are not specific features of taxis. Furthermore, effectively identical klinokinesis mechanisms have been advanced to explain bacterial attraction (18, 19) and chemotaxis in leukocytes and *Dictyostelium*. It was proposed (9, 31) that taxis results from a temporal, adaptive mechanism existing in pseudopods that probe the environment. Correctly aligned pseudopods would be promoted and others inhibited, much as the random (klinokinetic-adaptive) directional "probes" of swimming bacteria. However, these conclusions (9, 31) were based on experiments in which cells were probably exposed to stimulant impulses. (We postulate that taxis might be mediated by this mechanism only if pseudopod activity is coordinated or integrated.)

Absolutely defined, static spatial gradients can be made by binding stimulant molecules to the substratum (62–65). The accumulation of fibroblasts that occurs on palladium gradients was termed "haptotaxis" (62). However, cells move seemingly randomly and do not become aligned during the reaction (65), indicating that the cell response is probably chemokinetic, not tactic. The presence or absence of adaptation, which might have caused the accumulation, may be tested directly.

Effects of Stimulant Impulses

An impulse effect consists of (*a*) the initial contact between one part of the cell and the stimulant, which might, indeed, induce a pioneer pseudopod at that point (66) and (*b*) the less rapidly developing spatial and temporal gradient about the cell, which probably has no directional information above that of a spatial gradient. van Haastert et al. (29) reported that the maximal intracellular cyclic guanosine monophosphate synthesis occurs within 10 s of the reception of a cAMP impulse, and some synthesis may be localized beneath the plasmalemma. 50% occupation of the cyclic guanosine monophosphate binding protein requires the addition of $\sim 10^{-10}$ M cAMP to cells, but 50% occupation of the cell surface cAMP receptors requires 10^{-8} to 10^{-7} M, the level at which we obtain maximal chemoattraction and migration. Possibly, the low cAMP concentration of the leading "edge" of a developing gradient is sufficient to stimulate (*a*) a brief adaptive response and (*b*) the production of a directed pseudopod at the first point of contact with a cell, which polarizes it and might, thus, determine chemotaxis. The subsequent higher concentrations in the ensuing spatial gradient enhance biased-random locomotion. We have calculated that the leading edge of a developing gradient may move across a cell in, roughly, between 0.5 and 5 s.

In nature, *D. discoideum* avoids the fate of random, equilibrium population distribution, because the autonomous emission of cAMP by each cell is dominated by its rhythmic, pulsatile excretion and fine spatial and temporal modulation due to PDE (7, 21–24, 29, 42, 43)—the cells aggregate. Naturally and artificially delivered cAMP pulses also induce aggregation (67), cAMP and PDE excretion (21), oriented pseudopod projection (3, 9), chemotaxis (3, 50), and morphogenesis (6, 68). Rapid cAMP concentration increases stimulate a subplasma membrane reaction within seconds (29, 69, 70).

Several of these cell responses to cAMP are adaptive; i.e., cAMP excretion (21) and localized subplasmalemmal cGMP synthesis and binding (29), which are different responses with perhaps differing significance for chemotaxis (29). Only rapid stimulant concentration increases (impulses) polarize leukocytes (31, 71) and cause transmembrane potential changes and ion influxes (25).

Continuous adaptive response occurred in myxamoebae exposed to a stepwise series of 25 cAMP concentration increases 90 s apart, from 10^{-12} to 10^{-5} M, within ~32 min (see Fig. 9 in reference 21). Compare this effect of a temporal gradient to our observations of cells translocating smooth, static spatial gradients and encountering values from ~0 to 10^{-6} M cAMP in not less than 15 min. Although the time and concentration values are similar between the two experiments, accumulation did not occur in spatial gradients presumably because of the absence of locomotory adaptation. Adaptation drives attraction and accumulation in randomly swimming bacteria (19, 72). In leukocytes and myxamoebae, contraction accompanies the application of a stimulant gradient or a pulse (3, 30, 73), but does not recur as either cell type advances up the succeeding spatial gradient. Thus, only temporal gradients may induce adaptation responses (see also references 50 and 61) and, perhaps, directed pseudopods (9, 31).

Combined Speed and Persistence Effects in Kinesis

Fig. 5 demonstrates a cAMP concentration optimum for attraction. Why should cells in gradients not advance toward that optimum irrespective of its direction up- or down-gradient? Cells must then read the direction of the gradient; we reject this explanation, because populations assume even distributions when confined in gradients. Furthermore, if cells in fact read $\Delta c/c$, then the value in a linear gradient would decrease nearer the source; cells might tend to loosely accumulate somewhere in the middle of the gradient territory, yet this does not occur.

We suspect that cAMP affects both cellular speed and persistence, producing a composite, average behavior. A simple, but not unique, assumption is that speed increases linearly with cAMP concentration while persistence increases, then declines after a particular concentration. Different hypothetical combinations of speed and persistence effects could lead to other results.

Morphogen Gradients in Development

Linear spatial morphogen gradients (11, 16, 74, 75) are thought to deliver positional rather than directional information. Nevertheless, spatial gradients will be uninterpretable by cells if they depend only on a concentration-reading mechanism matching the one that we have demonstrated for myxamoeba. A possible example of a morphogen gradient in development might be nematocyte migration in hydra (76). The resemblance of the attraction distribution pattern of *Dictyostelium* to that of the nematocytes leads us to consider the latter in terms of a chemokinetic, rather than a chemotactic, reaction to a morphogen gradient. The accumulation of nematocytes in tentacles might result from adaptation or from an additional mechanism.

One way cells may overcome their individual biased-random responses to spatial gradients and generate orderly patterns is by integration. This might be possible by temporal (16) or spatial means. Interestingly, *Dictyostelium* cells become integrated during morphogenesis by cohesion and contact following (1, 77), which helps reduce directional errors. Therefore, we thought it likely that, in other developing organisms as well, the concentration patterns of information in spatial gradients of morphogens might only become available if neighboring cells integrate themselves (i.e., their stochastic responses) into larger functional units of a few cells. The resolution of the signal would decrease, but at a gain of positional accuracy. This integration might be mediated by intercellular small-gap junctions as their essential role. Dixon and Cronly-Dillon (78) have already suggested that small-gap junctions arise coincidentally with the proposed interval of morphogen signal transmission in the developing toad retina.

APPENDIX

Sample Characteristics for Grouped Data

We obtain data in form of

$$\ldots f_{-5} f_{-4} f_{-3} f_{-2} f_{-1} f_0 f_1 f_2 f_3 f_5 \ldots x \text{ axis},$$

where f_i indicates the frequency of cells in class i, each class having width b, d is the centre of class 0, n is the total number of cells, and S is the standard deviation.

$$\text{mean} = d + b\,\frac{(\sum f_i z_i)}{n} \tag{1}$$

$$\text{median} = \hat{u} + b\,\frac{\left(\frac{n}{2} - (\sum f)_{\hat{u}}\right)}{f_{\text{median}}} \tag{2}$$

$$S = \sqrt{b^2\,\frac{\sum fz^2 - (\sum fz)^2/n}{n-1}} \tag{3}$$

$$\text{Skew} = \frac{b^3}{S^3}\left(\frac{\sum fz^3}{n} - \left(3\,\frac{\sum fz^2}{n}\right)\cdot\left(\frac{\sum fz}{n}\right) + 2\left(\frac{\sum fz}{n}\right)^3\right) \tag{4}$$

In Eq. 2 $\hat{u}$ = lower limit of the median class, $(\sum f)_{\hat{u}}$ = sum of cells below the median class, and f_{median} = sum of cells in the median class.

Wilcoxon Signed Rank Test

$$R = \sum_{i>0} \text{Sgn}(R_i)\cdot R_i,$$

where R_i is the mean rank of the classes $Z = +i$, $Z = -i$; i.e., R is the sum of positive ranks. Under the null-hypothesis (median = 0), the expected value of R is

$$E(R) = (n\cdot(n+1) - f_0\cdot(f_0+1))/4$$

and the variance of R is

$$\text{Var} = [n\cdot(n+1)\cdot(2n+1) - f_0\cdot(f_0+1)\cdot(2f_0+1)]/24 - \sum_{i>0} f_i\cdot(f_i+1)\cdot(f_i-1)/48$$

Then,

$$X\text{norm} = \frac{R - E(R)}{\sqrt{\text{Var}}}$$

is an asymptotically normal variable with mean zero and variance = 1.

We are deeply grateful to G. Gerisch (Martinsried), B. Jastorff (Bremen), P. J. M. van Haastert (Leiden), and T. M. Konijn (Leiden) for amoebae, mutants, advice, and discussions and to V. D. Gooch

(Morris, Minnesota) and T. M. Konijn for reading the manuscript. We are indebted to H. Schwegler (Bremen) for the water container analogy and to Annegret Tin for typing.

Received for publication 7 June 1983, and in revised form 8 February 1984.

REFERENCES

1. Bonner, J. T. 1947. Evidence for the formation of cell aggregates by chemotaxis is the development of the slime mold *Dictyostelium discoideum*. *J. Exp. Zool.* 106:1–26.
2. Darmon, M., J. Barra, and P. Brachet. 1978. The role of phosphodiesterase in aggregation of *Dictyostelium discoideum*. *J. Cell Sci.* 31:233–243.
3. Futrelle, R. P., J. Traut, and W. G. McKee. 1982. Cell behavior in *Dictyostelium discoideum*: preaggregation response to localized cyclic AMP pulses. *J. Cell Biol.* 92:807–821.
4. Gerisch, G. 1968. Cell aggregation and differentiation in *Dictyostelium*. *Curr. Top. Dev. Biol.* 3:157–197.
5. Klein, C. 1975. Induction of phosphodiesterase by cyclic adenosine 3′:5′-monophosphate in differentiating *Dictyostelium discoideum* amoeba. *J. Biol. Chem.* 250:7134–7138.
6. Mangiarotte, G., A. Ceccarelli, and H. F. Lodish. 1983. Cyclic AMP stabilizes a class of developmentally regulated *Dictyostelium discoideum* mRNA's. *Nature (Lond.).* 301:616–618.
7. Shaffer, B. M. 1975. Secretion of cyclic AMP induced by cyclic AMP in the cellular slime mould *Dictyostelium discoideum*. *Nature (Lond.).* 255:549–552.
8. Swanson, J. A., and D. L. Taylor. 1982. Local and spatially coordinated movements in *Dictyostelium discoideum* amoeba during chemotaxis. *Cell.* 28:225–232.
9. Gerish, G., D. Huelser, D. Malchow, and U. Wick. 1975. Cell communication by periodic cyclic-AMP pulses. *Philos. Trans. R. Soc. Lond. B. Biol. Sci.* 272:181–192.
10. Weiss, P. 1936. Principles of Development. Holt, Reinhart & Winston Inc., New York. 601 pp.
11. Crick, F. 1970. Diffusion in embryogenesis. *Nature (Lond.).* 225:420–422.
12. Wolpert, L. 1969. Positional information and the spatial pattern of cellular differentiation. *J. Theor. Biol.* 25:1–47.
13. Futrelle, R. P. 1982. *Dictyostelium* chemotactic response to spatial and temporal gradients: theories of the limits of chemotactic sensitivity and of pseudochemotaxis. *J. Cell. Biochem.* 18:197–212.
14. Mato, J. M., A. Losada, N. Nanjundiah, and T. M. Konijn. 1975. Signal input for a chemotactic response in the cellular slime mold *Dictyostelium discoideum*. *Proc. Natl. Acad. Sci. USA.* 72:4991–4993.
15. Ramsey, W. S. 1974. Retraction fibers and leukocyte chemotaxis. *Exp. Cell Res.* 86:184–186.
16. Berg, H. C., and E. M. Purcell. 1977. Physics of chemoreception. *Biophys. J.* 20:193–219.
17. Keller, H. U., and M. Bessis. 1975. Migration and chemotaxis of cytoplasmic leukocyte fragments. *Nature (Lond.).* 258:723–724.
18. Berg, H. C., and D. A. Brown. 1974. Chemotaxis in *Escherichia coli* analyzed by three-dimensional tracking. *Antibiot. Chemother. (Basel).* 19:55–78.
19. MacNab, R. M., and D. E. Koshland, Jr. 1972. The gradient-sensing mechanism in bacterial chemotaxis. *Proc. Natl. Acad. Sci. USA.* 69:2509–2512.
20. Devreotes, P. N., P. L. Derstine, and T. L. Steck. 1979. Cyclic 3′,5′ AMP relay in *Dictyostelium discoideum*. I. A technique to monitor responses to controlled stimuli. *J. Cell Biol.* 80:291–299.
21. Devreotes, P. N., and T. L. Steck. 1979. Cyclic 3′,5′ AMP relay in *Dictyostelium discoideum*. II. Requirements for initiation and termination of the response. *J. Cell Biol.* 80:300–309.
22. Dinauer, M. C., S. A. MacKay, and P. N. Devreotes. 1980. Cyclic 3′,5′ AMP relay in *Dictyostelium discoideum*. III. The relationship of cAMP synthesis and secretion during the cAMP signalling response. *J. Cell Biol.* 86:535–544.
23. Dinauer, M. C., T. L. Steck, and P. N. Devreotes. 1980. Cyclic 3′,5′ AMP relay in *Dictyostelium discoideum*. IV. Recovery of the cAMP signalling response after adaptation to cAMP. *J. Cell Biol.* 86:545–553.
24. Dinauer, M. C., T. L. Steck, and P. N. Devreotes. 1980. Cyclic 3′,5′ AMP relay in *Dictyostelium discoideum*. V. Adaptation of the cAMP signalling response during cAMP stimulation. *J. Cell Biol.* 86:554–561.
25. Gallin, E. K., and J. I. Gallin. 1977. Interaction of chemotactic factors with human macrophages: induction of transmembrane potential changes. *J. Cell Biol.* 75:277–289.
26. Gerisch, G., and B. Hess. 1974. Cyclic-AMP controlled oscillations in suspended *Dictyostelium* cells: their relation to morphogenetic cell interactions. *Proc. Natl. Acad. Sci. USA.* 71:2118–2122.
27. O'Flaherty, J. T., D. L. Kreutzer, and P. A. Ward. 1977. Neutrophil aggregation and swelling induced by chemotactic agents. *J. Immunol.* 119:232–239.
28. Sklar, L. A., A. J. Jesaitas, R. G. Painter, and C. G. Cochraine. 1981. The kinetics of neutrophil activation. *J. Biol. Chem.* 256:9909–9914.
29. van Haastert, P. J. M., H. van Walsum, and F. J. Pasveer. 1982. Nonequilibrium kinetics of a cyclic GMP-binding protein in *Dictyostelium discoideum*. *J. Cell Biol.* 94:271–278.
30. Zigmond, S. H., and S. J. Sullivan. 1979. Sensory adaptation of leukocytes to chemotactic peptides. *J. Cell Biol.* 82:517–527.
31. Gerisch, G., and H. U. Keller. 1981. Chemotactic reorientation of granulocytes stimulated with micropipettes containing fMet-Leu-Phe. *J. Cell Sci.* 52:1–10.
32. Zigmond, S. H. 1974. Mechanisms of sensing chemical gradients by polymorphonuclear leukocytes. *Nature (Lond.).* 249:450–452.
33. Zigmond, S. H. 1977. Ability of polymorphonuclear leukocytes to orient in gradients of chemotactic factors. *J. Cell Biol.* 75:606–616.
34. Zigmond, S. H. 1978. Chemotaxis of polymorphonuclear leukocytes. *J. Cell Biol.* 77:269–287.
35. Keller, H. U., P. C. Wilkinson, M. Abercrombie, E. L. Becker, J. G. Hirsch, M. L. Miller, S. Ramsey, and S. Zigmond. 1977. A proposal for the definition of terms related to locomotion of leukocytes and other cells. *J. Immunol.* 118:1912–1914.
36. Fraenkel, G. S., and D. L. Gunn. 1961. The Orientation of Animals; Kinesis, Taxes and Compass Reactions. Dover, New York. 334 pp.
37. Konijn, T. M., and K. B. Raper. 1961. Cell aggregation in *Dictyostelium discoideum*. *Dev. Biol.* 3: 725–756.
38. Vicker, M. G. 1981. Ideal and non-ideal concentration gradient propagation in chemotaxis studies. *Exp. Cell Res.* 136:91–100.
39. Sternfeld, J., and C. N. David. 1981. Oxygen gradients cause pattern orientation in *Dictyostelium* cell clumps. *J. Cell Sci.* 50:9–17.
40. Zigmond, S. H. 1974. A modified millipore filter method for assaying polymorphonuclear leukocyte locomotion and chemotaxis. *Antibiot. Chemother. (Basel).* 19:126–145.
41. Gerisch, G. 1976. Extracellular cyclic-AMP phosphodiesterase regulation in agar plate cultures of *Dictyostelium discoideum*. *Cell Differ.* 5:21–25.
42. Malchow, D., and G. Gerisch. 1974. Short term binding and hydrolysis of cyclic 3′,5′-adenosine monophosphate. *Proc. Natl. Acad. Sci. USA.* 58:1152–1154.
43. Roos, W., D. Malchow, and G. Gerisch. 1975. Adenyl cyclase and the control of cell differentiation in *Dictyostelium discoideum*. *Cell Differ.* 6:229–239.
44. Pannbacker, R. G., and L. J. Bravard. 1972. Phosphodiesterase in *Dictyostelium discoideum* and the chemotactic response to cyclic adenosine monophosphate. *Science (Wash. DC).* 175:1014–1015.
45. Rossier, C., E. Eitle, R. van Driel, and G. Gerisch. 1980. Biochemical regulation of cell development and aggregation in *Dictyostelium discoideum*. *In* The Eukaryotic Cell. G. W. Gooday, D. Lloyd, and A. P. J. Trinci, editors. Cambridge University Press, Cambridge. 405–424.
46. Mason, J. W., H. Rasmussen, and F. DiBella. 1971. 3′,5′ AMP and Ca^{2+} in slime mold aggregation. *Exp. Cell Res.* 67:156–160.
47. Klein, C. 1981. The binding of adenosine 3′:5′-monophosphate to plasma membranes of *Dictyostelium discoideum* amoeba. *J. Biol. Chem.* 256:10050–10053.
48. Nelson, R. D., R. T. McCormack, and V. D. Fiegel. 1978. Chemotaxis of human leukocytes under agarose. *In* Leukocyte Chemotaxis. J. I. Gallin, and P. Q. Quie, editors. Raven Press, New York. 25–40.
49. Tono-Oka, T., M. Nakayama, and S. Matsumoto. 1978. Enhanced granulocyte mobility by chemotactic factor in the agarose plate. *Proc. Soc. Exp. Biol. Med.* 159:75–79.
50. Konijn, T. M. 1970. Microbiological assay of cyclic 3′:5′-AMP. *Experentia (Basel).* 26:367–369.
51. Maksukama, S., and A. J. Durston. 1979. Chemotactic cell sorting in *Dictyostelium discoideum*. *J. Embryol. Exp. Morphol.* 50:243–251.
52. Potel, M. K., and S. A. MacKay. 1979. Preaggregative cell motion in *Dictyostelium*. *J. Cell Sci.* 36:281–309.
53. Rosen, G. 1976. Chemotactic transport theory for neutrophil leukocytes. *J. Theor. Biol.* 59:371–380.
54. Tomchik, K. J., and P. N. Devreotes. 1981. Adenosine 3′,5′-monophosphate waves in *Dictyostelium discoideum*: a demonstration by isotope dilution-fluorography. *Science (Wash. DC).* 212:443–446.
55. Lapidus, I. R. 1980. "Pseudochemotaxis" by micro-organisms in an attractant gradient. *J. Theor. Biol.* 86:91–103.
56. Parnas, H., and L. A. Segel. 1977 Computer evidence concerning the chemotactic signal in *Dictyostelium discoideum*. *J. Cell Sci.* 25:191–204.
57. Zigmond, S. H., and J. G. Hirsch. 1973. Leukocyte locomotion and chemotaxis: new methods for evaluation and demonstration of a cell-derived chemotactic factor. *J. Exp. Med.* 137:387–410.
58. Oliver, J. M. 1978. Cell biology of leucocyte abnormalities—membrane and cytoskeletal function in normal and defective cells. *Am. J. Pathol.* 93:221–259.
59. Letourneau, P. C. 1978. Chemotactic response of nerve fiber elongation to nerve growth factor. *Dev. Biol.* 66:183–196.
60. Futrelle, R. P., and H. C. Berg. 1972. Specification of gradients used for studies of chemotaxis. *Nature (Lond.).* 239:517–518.
61. McCutcheon, M. 1946. Chemotaxis in leukocytes. *Physiol. Rev.* 26:319–336.
62. Carter, S. B. 1967. Haptotaxis and the mechanism of cell motility. *Nature (Lond.).* 213:256–260.
63. Dierich, M. P., D. Wilhelmi, and G. Till. 1977. Essential role of surface-bound chemoattractant in leucocyte migration. *Nature (Lond.).* 270:351–352.
64. Wilkinson, P. C., and R. B. Allan. 1978. Chemotaxis of neutrophil leukocytes towards substratum-bound protein attractants. *Exp. Cell Res.* 117:403–412.
65. Harris, A. 1974. Behavior of cultured cells on substrata of variable adhesiveness. *Exp. Cell Res.* 77:285–297.
66. Cohen, M., and A. Robertson. 1971. Chemotaxis and the early stages of aggregation in cellular slime molds. *J. Theor. Biol.* 31:119–130.
67. Robertson, A., D. J. Drage, and M. H. Cohen. 1972. Control of aggregation in *Dictyostelium discoideum* by an external periodic pulse of cyclic adenosine monophosphate. *Science (Wash. DC).* 175:333–335.
68. Darmon, M., P. Brachet, and L. H. Pereira Da Silva. 1975. Chemotactic signals induce cell differentiation in *Dictyostelium discoideum*. *Proc. Natl. Acad. Sci. USA.* 72:3163–3166.
69. Green, A. A., and P. C. Newell. 1975. Evidence for the existence of two types of cAMP binding sites in the aggregating cells of *Dictyostelium discoideum*. *Cell.* 6:129–136.
70. Henderson, E. J. 1975. The cyclic adenosine 3′:5′-monophosphate receptor of *Dictyostelium discoideum*. *J. Biol. Chem.* 250:4730–4736.
71. Malech, H. L., R. K. Root, and J. I. Gallin. 1977. Structural analysis of human neutrophil migration. *J. Cell Biol.* 75:666–693.
72. Berg, H. C., and P. M. Tedesco. 1975. Transient response to chemotactic stimuli in *Escherichia coli*. *Proc. Natl. Acad. Sci. USA.* 72:3235–3239.
73. Gerisch, G., and D. Malchow. 1976. Cyclic-AMP receptors and the control of cell aggregation in *Dictyostelium*. *Adv. Cyclic Nucleotide Res.* 7:49–68.
74. Child, C. M. 1928. The physiological gradients. *Protoplasma.* 5:447–476.
75. Meinhardt, H., and A. Gierer. 1974. Applications of a theory of biological pattern formation based on lateral inhibition. *J. Cell Sci.* 15:321–346.
76. Campbell, R. D., and B. A. Marcum. 1980. Nematocyst migration in hydra: evidence for contact guidance *in vivo*. *J. Cell Sci.* 41:33–51.
77. Klaus, M., and R. P. George. 1974. Microdissection of developmental stages in the cellular slime mould *Dictyostelium discoideum*, using a ruby laser. *Dev. Biol.* 39:183–188.
78. Dixon, J. S., and J. R. Cronly-Dillon. 1972. The fine structure of the developing retina in *Xenopus laevis*. *J. Embryol. Exp. Morphol.* 28:659–666.